Paracrine rescue of MYR1-deficient *Toxoplasma gondii* mutants reveals limitations of pooled *in vivo* CRISPR screens

Francesca Torelli [1,2,§], Diogo M. da Fonseca [1,2,§], Simon Butterworth [1,a], Joanna C. Young [1,b], Moritz Treeck [1,2,*]

[§] These authors contributed equally

[1] Signalling in Apicomplexan Parasites Laboratory, The Francis Crick Institute, London, UK NW1 1AT
[2] Host-Pathogen Interactions Laboratory, GIMM - Gulbenkian Institute for Molecular Medicine, 1649-025, Lisbon, Portugal
[a] Current address: Whitehead Institute, Massachusetts Institute of Technology, Cambridge, MA 02142-1479, USA
[b] Current address: Institute of Immunology and Infection Research, University of Edinburgh, Edinburgh, UK EH9 3FL

[*] Correspondence and requests for materials should be addressed to M.T. (moritz.treeck@gimm.pt)

Classifications: Biological Sciences/Microbiology
Keywords: CRISPR-Cas9 screen, *Toxoplasma gondii*, MYR1, host-pathogen interaction, paracrine effect

ABSTRACT

Toxoplasma gondii is an intracellular parasite that subverts host cell functions via secreted virulence factors. Up to 70% of parasite-controlled changes in the host transcriptome rely on the MYR1 protein, which is required for the translocation of secreted proteins into the host cell. Mice infected with MYR1 knock-out (KO) strains survive infection, supporting a paramount function of MYR1-dependent secreted proteins in *Toxoplasma* virulence and proliferation. However, we have previously shown that MYR1 mutants have no growth defect in pooled *in vivo* CRISPR-Cas9 screens in mice, suggesting that the presence of parasites that are wild-type at the *myr1* locus in pooled screens can rescue the phenotype. Here, we demonstrate that MYR1 is not required for the survival in IFN-γ-activated murine macrophages, and that parasites lacking MYR1 are able to expand during the onset of infection. While ΔMYR1 parasites have restricted growth in single-strain murine infections, we show that the phenotype is rescued by co-infection with wild-type (WT) parasites *in vivo,* independent of host functional adaptive immunity or key pro-inflammatory cytokines. These data show that the major function of MYR1-dependent secreted proteins is not to protect the parasite from clearance within infected cells. Instead, MYR-dependent proteins generate a permissive niche in a paracrine manner, which rescues ΔMYR1 parasites within a pool of CRISPR mutants in mice. Our results highlight an important limitation of otherwise powerful *in vivo* CRISPR screens and point towards key functions for MYR1-dependent *Toxoplasma*-host interactions beyond the infected cell.

SIGNIFICANCE STATEMENT

Pooled CRISPR screens are powerful tools to interrogate gene function in a high-throughput manner. Genes conferring fitness advantages or disadvantages upon disruption can be identified by sequencing. However, in *Toxoplasma gondii* pooled CRISPR screens in mice, fitness defects for some selected mutants drastically diverge from those observed in single-strain infections. Here, we show that a growth defect of a single *Toxoplasma* gene deletion mutant is rescued if co-infected with wildtype parasites. These results shine light on *Toxoplasma*'s ability to subvert the host response beyond the infected cell, and highlight an important limitation of pooled CRISPR screens in mice. This limitation is probably encountered in CRISPR screens in general where paracrine effects occur.

INTRODUCTION

Pooled CRISPR screens have been an extraordinarily powerful genetic tool to identify gene function in an unbiased manner using negative or positive selection. They have been applied in various cell culture conditions and *in vivo*, in combination with different genetic or chemical bottlenecks to identify genes in a specific setting (1). Fitness-conferring genes are identified by assessing the relative abundance of cells with different genetic perturbations within a pool of mutants upon selective pressure.

We have previously performed pooled CRISPR screens in mice with the intracellular parasite *Toxoplasma gondii*, to identify exported parasite proteins that are important for survival in his natural host (2, 3). For the majority of tested genes, the phenotypes observed in pooled CRISPR screens are concordant to those observed in single-strain infections using clonal mutants for those genes. To our surprise, however, we found that while some *Toxoplasma* genes are required for survival in single-strain mutant KO murine infections, this fitness defect phenotype is lost when the same mutants are part of a heterogenous mutant pool used for CRISPR screens in mice. We hypothesised that individual mutants can be rescued by paracrine effects triggered by other parasites in the pool, pointing towards a potential limitation of pooled CRISPR screens to detect a subset of important virulence factors in *Toxoplasma.* This limitation likely is not restricted to *Toxoplasma*, or other infectious contexts, but CRISPR screens in general where paracrine effects are operating.

Toxoplasma is a ubiquitous parasitic pathogen in all warm-blooded animals. *Toxoplasma* infection is widespread in livestock and wild animals, as well as in humans, where one third of the population is estimated to be seropositive (4). Following oral infection by oocysts or latent stage tissue cysts, the parasite grows as tachyzoites in

intermediate hosts, before disseminating to distal organs. The host immune response is pivotal to reduce parasite burden caused by rapidly proliferating tachyzoites. However, it is not sufficient to completely clear infection, as surviving parasites can differentiate into the chronic bradyzoite forms and establish tissue cysts in the central nervous system and skeletal muscle cells (5). During the onset of infection, recognition of *Toxoplasma*-derived pathogen-associated molecular patterns (PAMPs) by host innate immune cells triggers the production of IL-12, amongst other pro-inflammatory mediators (6). IL-12 has a protective role during toxoplasmosis, primarily by triggering IFN-γ production in lymphocytes and thereby linking innate and adaptive immunity during infection (7). IFN-γ is a pivotal cytokine in conferring resistance against *Toxoplasma* infection since it induces expression of interferon-stimulated genes (ISGs) that limit intracellular parasite proliferation and curtail infection (8–10). These antimicrobial effects are enhanced by other pro-inflammatory cytokines. An example is TNF, which acts as a co-stimulatory signal to trigger IFN-γ production by NK cells exposed to the parasite, and boosts the antimicrobial activity of IFN-γ-activated macrophages (11–13). Following *Toxoplasma* infection, host cells can also secrete chemokines such as CCL2, which drives recruitment of $CCR2^{+}Ly6C^{high}$ inflammatory monocytes from the bone marrow to the infected sites (14, 15). There, they can differentiate into monocyte-derived dendritic cells or macrophages and act as an extra line of defence against the parasite (16, 17).

In order to survive clearance by host immune cells and to disseminate within the infected host, *Toxoplasma* relies on an array of over 250 secreted proteins (18). Following invasion, *Toxoplasma* replicates inside a parasitophorous vacuole (PV) separated from the host cytoplasm by the PV membrane (PVM). During and after host cell invasion, *Toxoplasma* secretes proteins from the rhoptries and the dense granules. Secreted proteins from these organelles are not only pivotal for vacuole establishment, but also nutrient uptake, reprogramming of the infected cell and protection against the host immune response (19) . In order to exert their effect, some *Toxoplasma* proteins secreted from dense granules must cross the PVM, likely via a multi-protein translocon that depends on MYR1 (20). GRA16, a dense granule effector that relies on MYR-dependent export to exit the PV and reach the host cytosol, was shown to drive upregulation of the transcription factor c-Myc in host cells (21). After the identification of MYR1 other putative components of the MYR translocon – MYR2, MYR3, MYR4, ROP17 – were identified, using their ability to trigger GRA16-dependent c-Myc induction in infected cells as a surrogate (22–24). It was subsequently suggested that most, if not all exported dense granule proteins that reach the host cell cytosol might depend on functional MYR1 for translocation (23, 25). To date, seven virulence factors have been shown to be MYR1-dependent: IST, NSM, HCE1/TEEGR, GRA16, GRA18, GRA24 and GRA28. Once exported, these parasite proteins can interfere with host cell transcription and contribute to the establishment of permissive niches for *Toxoplasma* proliferation

and survival via multiple downstream mechanisms. Examples include boosting resistance against IFN-γ-dependent antimicrobial mechanisms (IST (26, 27)), arresting the host cell cycle (HCE1/TEEGR (28, 29)), inhibiting programmed host cell death pathways (NSM (30)) and modulating cytokine/chemokine secretion (GRA16, GRA18, GRA24, GRA28 (31–34).

Given the combined importance of exported dense granule effectors, it is not surprising that the vast majority of transcriptional changes in *Toxoplasma*-infected human fibroblasts are dependent on MYR1 (35), and that isogenic MYR1-deficient strains are avirulent in mice (20). In pooled *in vivo* CRISPR screens, however, we have shown that parasites lacking MYR1 had no fitness defect in a five-day infection experiment within the mouse peritoneum (2, 3). This is in agreement with results from *in vivo* CRISPR screens performed in other labs using different parasite strains and mouse backgrounds where no (25, 36), or only very mild growth defects (37) have been observed for MYR1. This divergence of results between isogenic infection, which clearly shows an important role for MYR1 in murine infections, and the pooled CRISPR screens, which show no defect of MYR1 mutants, led us to hypothesise that: 1) MYR1, and therefore proteins that rely on the MYR1 complex for translocation, are not essential for the cell-autonomous survival of parasites in macrophages, the main cell type infected in the first days of a peritoneal infection (38); and 2) ΔMYR1 parasites within a pool of mutants may be rescued by MYR1-competent parasites via a paracrine effect, setting up a parasite-permissive immune environment in which MYR1-deficient mutants can thrive.

Here, we verify both hypotheses, showing that MYR1 is not important for the *Toxoplasma* cell-autonomous survival within macrophages, and deploy co-infection strategies proving that MYR1-competent parasites can trans-rescue the growth defect of ΔMYR1 parasites *in vivo*. This rescue does not depend on the host adaptive immune response and surprisingly still occurs despite high levels of key pro-inflammatory cytokines. This knowledge is paramount to understand the biological function of MYR1-driven rewiring of the host cell, and consequently the function of MYR1-dependent effector proteins. It also highlights an important limitation of otherwise powerful *in vivo* pooled CRISPR screens in *Toxoplasma,* where loss-of-function of a protein in one parasite can be rescued by other parasites in the pool. This limitation likely extends to CRISPR screens in other biological contexts in which paracrine effects operate.

RESULTS

MYR1 is not essential for survival within IFN-γ-stimulated macrophages

To test whether MYR1 was required for the parasite cell-autonomous survival in immune cells, we infected IFN-γ-primed bone marrow-derived macrophages (BMDMs) with WT or MYR1 KO parasites established in the type II Prugniaud (Pru) genetic

background, and quantified infected cells after 24 h. As GRA12 was shown to be required for parasite survival in IFN-γ-stimulated macrophages (39) and had a strong growth defect in our pooled *in vivo* CRISPR screen (2), we included a ΔGRA12 strain in these experiments as positive control. As negative control, we included parasites lacking IST (SI Appendix, Fig. S1b), a known MYR1-dependent factor that inhibits the induction of interferon-stimulated genes. IST protects the parasites against intracellular restriction when the infection precedes IFN-γ activation, but not if *Toxoplasma* infects primed cells (26, 27). As expected, ΔGRA12 parasites showed a significant reduction in the proportion of infected cells in the presence of IFN-γ (Fig. 1a). Infection with ΔMYR1 was comparable to ΔIST and not significantly different to that of WT parasites, although a slight increase in restriction was observed for ΔIST and ΔMYR1. Our results are in line with findings from Wang and colleagues where deletion of MYR1 in a more virulent type I strain similarly causes no fitness defect in IFN-γ-activated macrophages (40).

To further validate the role of virulence factors in conferring parasite resistance against IFN-γ-mediated host defence, we assessed replication of ΔMYR1 or ΔGRA12 in competition with WT parasites over two lytic cycles in IFN-γ-treated or unprimed BMDMs, and in HFFs as control (Fig. 1b). As expected, ΔGRA12 was outcompeted by WT parasites exclusively in BMDMs pre-stimulated with IFN-γ, confirming its role to survive the cytokine-mediated clearance in macrophages (Fig. 1c). On the contrary, ΔMYR1 parasites displayed a fitness defect compared to WT parasites, regardless of the infected cell type and independently of IFN-γ treatment (Fig. 1c). This result is in line with the smaller size of the ΔMYR1 plaques established in HFFs compared to the parental strain (Fig. 1d), which recapitulates published data (22).

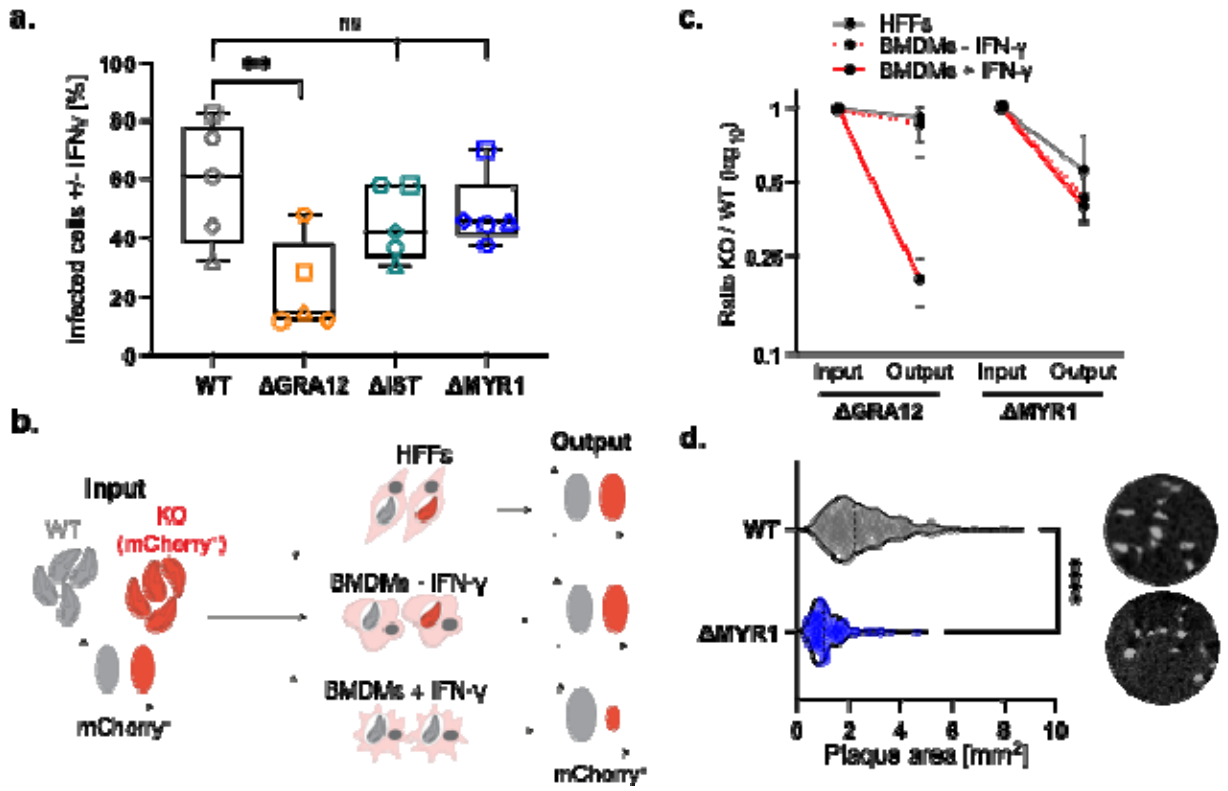

Fig 1. MYR1 and MYR1-dependent factors are not contributing to *in vitro Toxoplasma* survival in IFN-γ-activated macrophages. (a) BMDMs were stimulated with 100 U/ml IFN-γ for 24 h or left untreated, before infection with mCherry-expressing *Toxoplasma* strains for 24 h. Cells were fixed and imaged by high-content imaging, and the percentage of infected cells in IFN-γ-treated BMDMs compared to untreated controls is shown. WT refers to PruΔUPRT. The box-plot shows the median value and the whiskers show minimum and maximum values. Significance was tested with the One-way Anova test with the Benjamini, Krieger and Yekutieli FDR correction, n=5. (b) Schematic of the flow cytometer-based growth competition assay of an IFN-γ-dependent effector (e.g. GRA12). HFFs and BMDMs were co-infected with equal amounts of colourless WT and mCherry-expressing ΔGRA12 or ΔMYR1 strains. BMDMs were stimulated with 100 U/ml IFN-γ for 24 h or left untreated before infection. The mCherry signal was quantified by flow cytometry analysis and the ratio between the strains after two passages (output) was compared to the input. (c) Growth of competing mutant and WT parasites was assessed by flow cytometry. The normalised ratios of output versus input are shown. The average of two independent experiments with technical triplicates is shown. (d) Violin plot of the plaque size of parental PruΔKU80 and derived PruΔMYR1 strains. The bar represents the median value and representative images are reported on the right. Significance was tested using a two-tailed unpaired Welch's t-test, ** p<0.01, **** p<0.0001, n=2.

MYR1 mutants expand during the course of infection and can form tissue cysts *in vivo*

To investigate the growth of ΔMYR1 parasites *in vivo* and follow infection over time, we generated parasite strains expressing firefly luciferase (Luc) in the wild-type (WT-Luc) or ΔMYR1 backgrounds (ΔMYR1-Luc, SI Appendix Fig. S1c). We injected mice with 25,000 tachyzoites and monitored parasite growth over 7 days by intravital imaging (Fig.

2a). As expected from the reduced *in vitro* growth phenotype in HFFs and BMDMs, ΔMYR1-Luc showed reduced bioluminescent signal compared to WT-Luc parasites (Fig. 2b-c), confirming that the growth defect *in vitro* results in analogous phenotypes *in vivo*. Nevertheless, MYR1-deficient parasites were still able to expand in mice, as bioluminescence signal increased from day 3 to day 5 post infection (Fig. 2b-c). This initial increase of growth is similar to what was observed for ΔIST parasites (26, 27). ΔMYR1-Luc-infected mice that survived the acute phase of infection for four weeks p.i. carried a low number of cysts in the brain (3.4 cysts/brain on average; 0-13 cysts/brain detected, Fig. 1d). This is similar to previous observations (2) indicating that expression of luciferase does not decrease the ability to produce cysts and further supports the notion that ΔMYR1 parasites are able to form cysts, albeit at low numbers. As mice infected with WT parasites succumbed during the acute stage of infection, we cannot compare cyst numbers between the two strains.

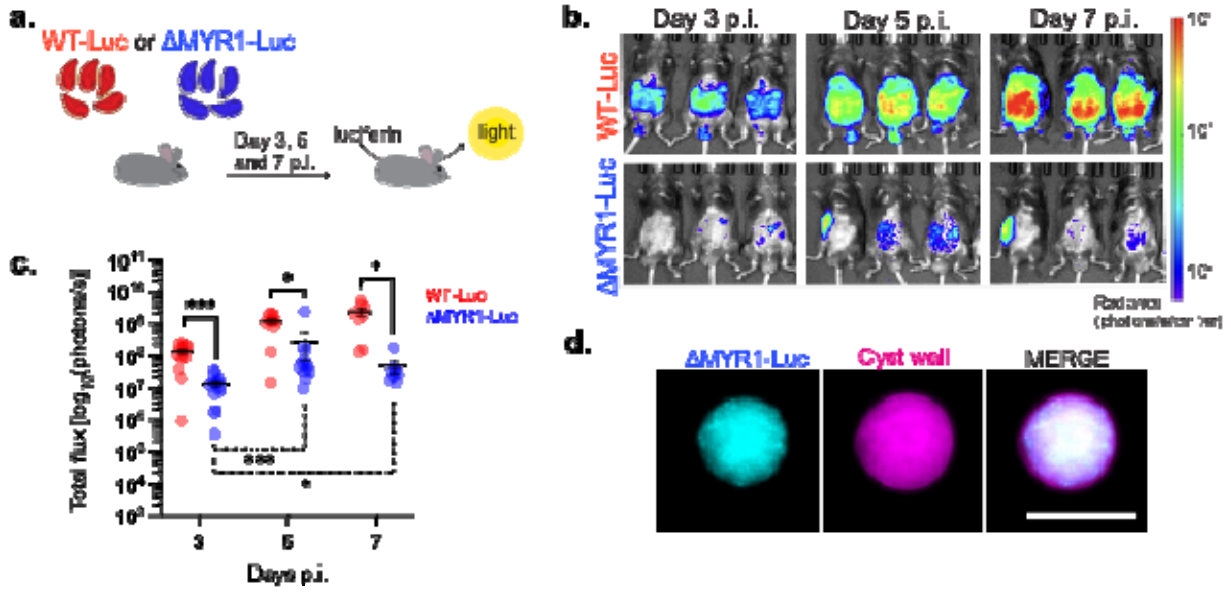

Fig. 2. ΔMYR1 parasites expand in the murine host and form cysts *in vivo*. (a) Mice were infected i.p. with luciferase-expressing *Toxoplasma* strains, WT-Luc or ΔMYR1-Luc, and whole-body intravital imaging was performed at days 3, 5 and 7 p.i. (b) Representative whole-body intravital imaging. (c) Graph shows the total bioluminescence signal converted to a logarithmic scale from two independent experiments. Statistical differences between the two strains at each timepoint were tested with the Mixed-effects model (REML) with Sidak post-hoc tests (continued lines). Significance for the ΔMYR1-Luc growth over time was tested with a One-Way Anova test (dotted line). Number of mice per group: day 3 p.i.: n=14; day 5 p.i.: n=11; day 7 p.i.: n=8. * p<0.05, *** p<0.001. (d) Representative fluorescent image of a brain cyst from a mouse infected with ΔMYR1-Luc. mCherry-expressing ΔMYR1-Luc parasites were detected by microscopy. Cyst wall was stained with the FITC-conjugated lectin DBA. The scale bar represents 25 µm.

MYR1-dependent secreted factor(s) rescue ΔMYR1 *in vivo* growth defect via a paracrine mechanism, independent of host adaptive immunity

We have shown that ΔMYR1 parasites have reduced *in vitro* and *in vivo* growth, despite not having any significant growth defect when in a pool with other mutants. Therefore, we hypothesised that MYR1-competent parasites within the KO pool generate a permissive environment that ultimately promotes growth of the ΔMYR1 mutants in a paracrine fashion. To test this hypothesis, we performed co-infection experiments where mice were injected with an inoculum containing a 20:80 ratio of ΔMYR1-Luc parasites with either WT parasites or ΔMYR1 mutants not expressing luciferase (Fig. 3a). This setting allows us to assess if the presence of WT parasites affects growth of ΔMYR1-Luc parasites within the peritoneum. Our results show that ΔMYR1-Luc parasites proliferate better in mice co-infected with WT parasites than with ΔMYR1 parasites (Fig. 3b-c). These results support a paracrine role of MYR1-mediated effectors *in vivo*.

To understand what mediates this trans-rescue phenotype, we assessed the production of selected pro-inflammatory cytokines important during *Toxoplasma* infection. Mice infected with a mix of ΔMYR1:WT or ΔMYR1:ΔMYR1 parasites display comparable levels of IL-12p40 in both peritoneum and serum at day 7 p.i. However, ΔMYR1:WT infections elicited higher levels of CCL2/MCP-1, TNF and especially IFN-γ compared to the ΔMYR1:ΔMYR1 mix (Fig. 3d, SI Appendix Fig. S1d-f).

Considering that ΔMYR1-Luc growth is rescued even when high levels of IFN-γ are produced in the peritoneal cavity, we wanted to assess whether disrupting IFN-γ-producing cell populations would impact the trans-rescue phenotype. Lymphocytes, in particular $CD8^+$, Th1-committed $CD4^+$ and γδ T cells, are the main sources of IFN-γ during *Toxoplasma* infection (41). Thus, we applied the same mixed infection strategy in Rag2-deficient mice that do not produce mature T and B cells, and therefore fail to deploy adaptive immune responses (42) (Fig. 3e). As expected, an overall higher parasitaemia was detected in *Rag2*$^{-/-}$ mice when compared to WT mice, due to the known role of the T and B cells to control infection. Nevertheless, in both *Rag2*$^{-/-}$ and WT control mice ΔMYR1-Luc parasites proliferate more when mixed with WT parasites than with ΔMYR1 parasites (Fig. 3f). These results confirm that the host adaptive response is not essential for the trans-rescue of MYR1-deficient *Toxoplasma* during acute infection.

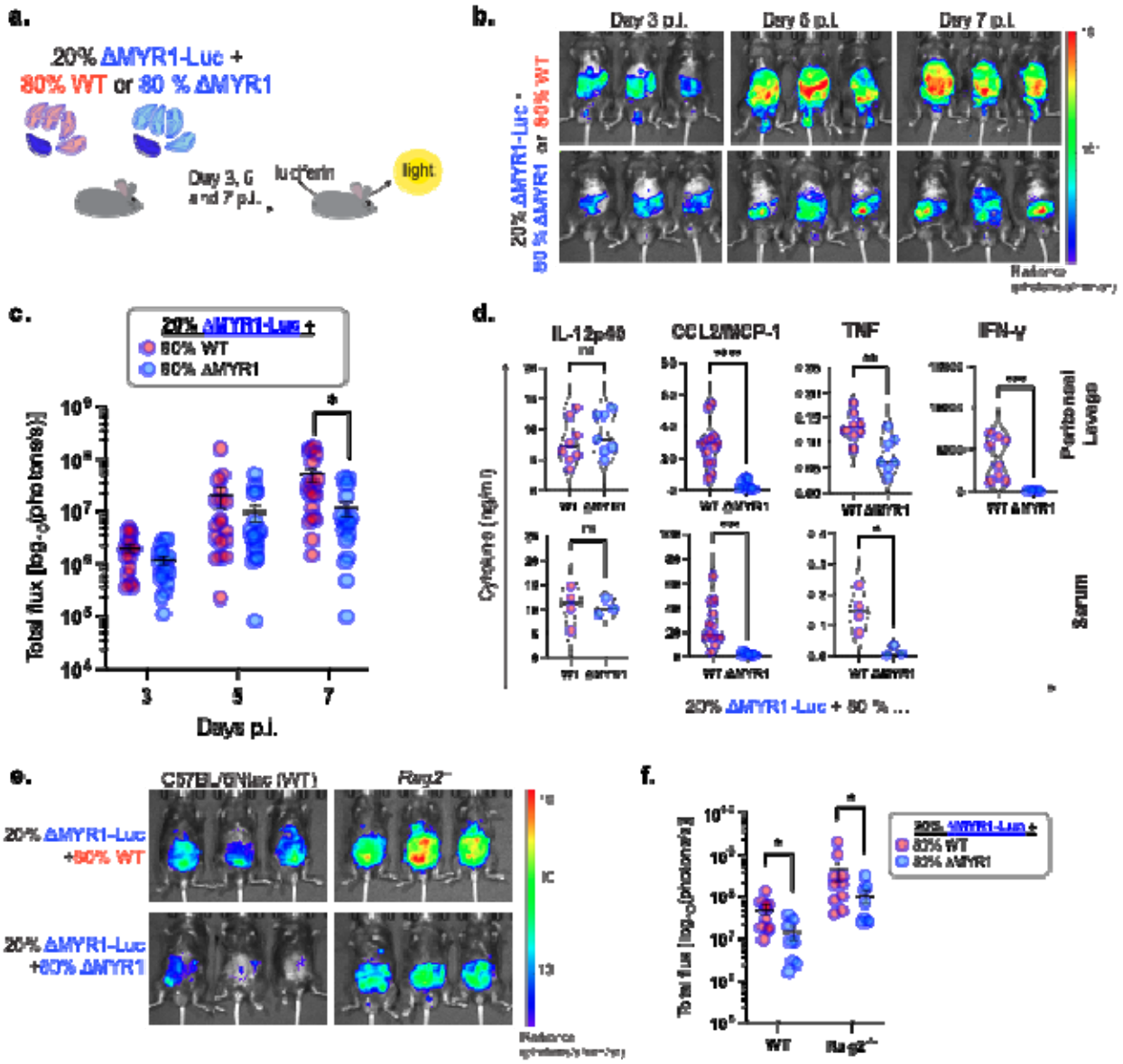

Fig 3. The *in vivo* growth defect of ΔMYR1 is rescued by the presence of MYR1-competent parasites, independently of functional host adaptive immunity. (a) Mice were infected i.p. with a mixed inoculum of *Toxoplasma* tachyzoites, containing a 20:80 ratio of luciferase-expressing ΔMYR1-Luc to WT or ΔMYR1 strains that do not express luciferase. Growth of ΔMYR1-Luc was monitored at 3, 5 and 7 days p.i. by whole-body intravital imaging. (b) Representative whole-body intravital imaging. (c) Total bioluminescence signal converted to a logarithmic scale from mice co-infected with ΔMYR1-Luc:WT (n=18) or ΔMYR1-Luc:ΔMYR1 (n=17). Graph shows cumulative data from four independent experiments. Significance was tested with a Two-way Repeated Measures ANOVA with Sidak post-hoc tests. (d) IL-12p40, CCL2/MCP-1, TNF and IFN-γ levels were detected in peritoneal lavage and serum of animals infected with mixed *Toxoplasma* inoculum (20:80 ratio) at day 7 p.i. by ELISA. The violin-plots show the median (continued black line) and quartiles (dotted grey lines). Significance was tested with the Welch's t-test (TNF, CCL2/MCP-1 and IL-12p40 ELISAs) and Mann-Whitney test (IFN-γ ELISAs). Samples from 2 to 3 independent experiments were assayed. Number of samples for CCL2: WT n=13 and ΔMYR1 n=12. Number of samples for other cytokines: peritoneal lavage samples: WT n=8 and ΔMYR1 n=7; serum samples: WT n=4 and ΔMYR1 n=3. Data with higher differences between inocula (CCL2 and IFN-γ) are

displayed in a logarithmic scale in SI Appendix Fig. S1d-f. (e) Representative whole-body intravital imaging at day 7 p.i. of C57BL/6Ntac (WT) or RAG2-deficient (*Rag2*$^{-/-}$) mice infected i.p. with a mixed inoculum containing a 20:80 ratio of luciferase-expressing ΔMYR1-Luc tachyzoites to WT or ΔMYR1 strains that do not express luciferase. (f) Total bioluminescence signal converted to a logarithmic scale from mice co-infected with ΔMYR1-Luc:WT (n=10) or ΔMYR1-Luc:ΔMYR1 (n=8). Graph shows cumulative data from two independent experiments. Significance was tested with the Multiple Mann-Whitney test with a False Discovery Rate approach by a Two-stage step-method. * p<0.05, ** p<0.01, *** p<0.001, **** p<0.0001.

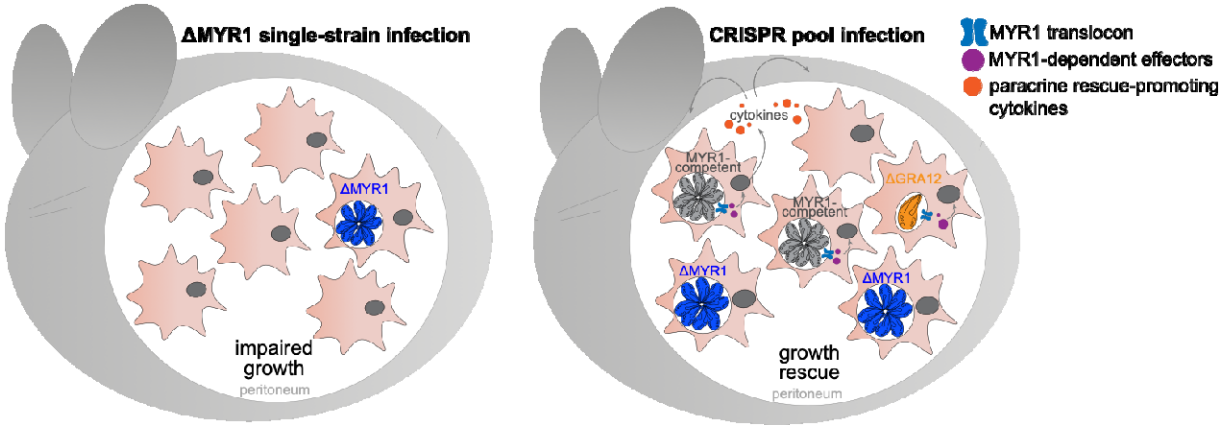

Fig 4. Model illustrating paracrine rescue of ΔMYR1 parasites in pooled CRISPR screens
Left panel: In single-strain infections ΔMYR1 parasites grow slowly within the peritoneum and are cleared. Right panel: Growth of ΔMYR1 parasites within a CRISPR pool is rescued by the presence of MYR-competent parasites. In cells infected with MYR1 competent parasites, MYR-dependent effectors enter the host cell, leading to secretion of cytokines that promote a favourable immune environment. MYR1 mutants are able to proliferate under these conditions (i.e are rescued *in trans*). However, *Toxoplasma* virulence factor mutants required for survival within a cell (cell-autonomous), such as GRA12, can not be rescued in trans.

DISCUSSION

In this work we show that deletion of MYR1, and by extension MYR1-dependent effectors, does not impact the ability of *Toxoplasma* to initiate an infection in mice and survive in IFN-γ-stimulated murine macrophages. While clonal ΔMYR1 mutants have a significantly reduced growth compared to WT parasites *in vivo*, co-infection with WT parasites increased their ability to proliferate. This finding supports results from pooled CRISPR-Cas9 screens, where loss-of-function mutants of *Myr1* and other genes previously shown to be involved in PV translocation of effector proteins, show no (2, 3, 25, 36) or only relatively minor fitness defects in mice (37). The rescue phenotype observed in mixed infections is very unlikely to occur through co-infection of host cells by WT and ΔMYR1 parasites, as in the peritoneal exudate from infected mice less than 2% of all infected cells were co-infected (data not shown). As such, our data indicates that some MYR1-dependent effectors cause changes in infected murine cells, that in turn provide a favourable environment for parasite growth in a paracrine manner. This is important as: 1) It shows that the major transcriptional changes caused by MYR-

dependent effectors are not required for *Toxoplasma* to survive cell-autonomous immune responses in IFN-γ-primed cells; 2) Paracrine rescue in pooled CRISPR-Cas9 screens may mask a significant amount of proteins required for *Toxoplasma* survival; 3) It is likely that this "paracrine masking effect" can be found in CRISPR screens in other biological contexts, e.g.: other host-microbe interaction screens, and possibly even in non-infectious biological contexts, such as pooled CRISPR screen approaches to study cancer immunity and to discover regulators of innate and adaptive immunity crosstalk (reviewed in (43, 44)).

We found that the presence of WT parasites in a mixed inoculum with ΔMYR1 mutants elicited significantly higher levels of IFN-γ and TNF in the peritoneum than ΔMYR1 mutants alone. As IFN-γ was shown to be a major cytokine to limit *Toxoplasma* growth in a cell-autonomous manner, and that TNF acts mainly by enhancing the antimicrobial effects in IFN-γ-activated cells, one would expect that ΔMYR1-Luc parasites would be more restricted when injected in combination with WT parasites. However, we observed the opposite, as higher ΔMYR1-Luc parasitaemia was observed in ΔMYR1:WT than in ΔMYR1:ΔMYR1 mixes. These data provide further support that MYR1, and by extension MYR1-dependent effectors, do not protect *Toxoplasma* from the IFN-γ-mediated intracellular clearance in mice.

What could be the driving force of the rescue? We show that the adaptive immune system plays no role, pointing towards cells of the innate immune system. Higher CCL2 levels in mice infected with ΔMYR1:WT suggests higher inflammatory Ly6C^{high} monocytes recruitment to infected tissues (14, 15). These cells could be responsible for the high levels of TNF and IFN-γ detected. While monocytes have been shown in multiple reports to be important for limiting *Toxoplasma* upon exposure to IFN-γ in infected niches (14, 17, 45), it is possible that recruited monocytes also provide an important reservoir for parasites to grow in the peritoneum. However, how ΔMYR1 parasites are eventually cleared in homogenous infections in the absence of high levels of CCL2 is not yet known.

Individual MYR-related effectors that may be responsible for the paracrine rescue have not been investigated here and we hypothesise that the phenotype is likely the concerted result of multiple effectors that affect cytokine secretion. For example, previous studies showed that both GRA18 and GRA28 can induce release of CCL22 from infected cells (32, 46), while GRA16 and HCE1/TEEGR impair NF-kB signalling and the potential release of pro-inflammatory cytokines such as IL-6, IL-1β and TNF (29, 47). Regardless of the effector(s), our results highlight an important novel function of MYR1-dependent effectors by establishing a supportive environment in *trans* for *Toxoplasma* growth within the peritoneum.

We further confirm previous results using luciferase-expressing ΔMYR1 parasites that MYR1 appears to be dispensable for the formation and persistence of latent *Toxoplasma* stages *per se*. As MYR1 has been demonstrated to be dispensable for stage conversion *in vitro* (48), the relatively low number of cysts is likely explained by a failure of ΔMYR1 parasites to efficiently disseminate and/or persist within the murine host (34). In alternative, we hypothesise that the absence of CCL2 in ΔMYR1 infections limits recruitment of host cells that *Toxoplasma* can potentially use as vehicles to reach the brain.

This work also highlights the limitations of restriction-based CRISPR-screens in capturing the variety of pathogen's mechanisms to survive host clearance. Novel applications of the CRISPR screens, for example in combination with single-cell RNA sequencing (49) or with functional assays to explore immunological contexts (43) could help understand how infected cells affect the neighbouring environment to support infection, and contribute to parasite survival, dissemination and persistence within the host. Here, we show that MYR1-dependent proteins play a critical role in promoting a favourable environment for growth beyond the infected cell in a paracrine manner. This is different to the injection of rhoptry effector proteins by *Toxoplasma* into cells it does not invade, which requires parasite-host cell contact (50), and provides a novel angle on how the parasite can systematically alter the host environment in its favour during infection.

Our work draws attention to an understudied aspect of pathogen manipulation in complex multicellular settings which warrants further studies. The limitation we highlight here, that mutant phenotypes can be masked in pooled CRISPR screens, likely extends to other experimental setups where paracrine effects are possible.

MATERIAL AND METHODS

Cell culture and parasite strains. Primary human foreskin fibroblasts (HFFs) (ATCC) were maintained in Dulbecco's modified Eagle's Medium (DMEM) with 4.5 g/L glucose and GlutaMAX-1 (Gibco Thermo Fisher Scientific) supplemented with 10% foetal bovine serum (FBS) (Gibco Thermo Fisher Scientific) at 37°C and 5% CO_2. To generate bone marrow-derived macrophages (BMDMs), bone marrow cells were extracted from femurs of C57BL/6J mice and differentiated to macrophages for 7 days at 37°C and 5% CO_2. Briefly, bone marrow cells were seeded in 15 cm^2 Petri dishes (Corning) and differentiated into BMDMs in RPMI 1640 medium (Gibco Thermo Fisher Scientific) supplemented with 20% L929 conditioned media (containing the murine macrophage colony stimulating factor (mM-CSF)), 50 µM *2*-mercaptoethanol, Penicillin/Streptomycin (Thermo Fisher Scientific), and 10% FBS. For experiments BMDMs were grown in the

above RPMI medium but lacking 2-mercaptoethanol (called working media further on). *Toxoplasma gondii* strains PruΔKU80 (51), PruΔUPRT::mCherry (3), PruΔGRA12::mCherry (2), PruΔMYR1::mCherry (2) and derived strains were maintained in confluent HFFs and passaged by syringe lysis through 23G needles every 2-3 days.

Generation of parasite lines. 10^6 freshly lysed parasites were transfected with 20-25 µg of DNA by electroporation using the 4D-Nucleofector (Lonza) with previously optimised protocols as described in Young *et al* (2). All primers used are listed in SI Appendix Fig. S1a. To generate pSAG1::Cas9sgIST the IST gRNA sequence was inserted into pSAG1::Cas9sgUPRT (52) by inverse PCR using primers 1&2. To generate the IST KO (PruΔIST::mCherry), PruΔKU80 parasites were co-transfected with pSAG1::CAS9sgIST and a Pro-GRA1::mCherry::T2A::HXGPRT::Ter-GRA2 construct amplified with primers 3&4 containing 40 bp homology regions to the 5′- and 3′- untranslated regions of IST (ToxoDB TGME49_240060). 24 h after transfection, 50 µg/ml Mycophenolic acid (Merck) and Xanthine (Sigma) (M/X) were added to select for integration, and a clonal culture was verified by PCR with primers 5-8. To generate Luciferase expressing parasite lines, PruΔKU80 or PruΔMYR1::mCherry were co-transfected with pSAG1::CAS9sgUPRT and PciI digested pUPRT-ffLucHA to insert a HA-tagged Firefly luciferase gene (LucHA) into the *Uprt* locus and establish WT-Luc and ΔMYR1-Luc strains respectively. To generate pUPRT-ffLucHA, the GRA1 promoter region and firefly Luciferase sequences were amplified from pGRA (53) and pDHFR-Luc (54) plasmids respectively using primers 9&10 and 11&12 and combined with BamHI/Xma digested pUPRT-HA in a Gibson reaction. 24 h post transfection 20 µg/ml FUDR (Sigma) was added to select for disruption of the *Uprt* locus and clones verified by PCR with primers 13&14.

Parasite growth in BMDMs. $5x10^4$ BMDMs were seeded per well in 96-well Ibitreat black µ-plates (Ibidi GmbH) in working media. The following day cells were either treated with IFN-γ (100 U/mL, Peprotech) or left untreated. 24 h later cells were infected with the strains in triplicate at a multiplicity of infection (MOI) of 0.3, and the plate was centrifuged at 210 *g* for 3 min. At 3 h post infection (p.i.) the medium was replaced to remove non-invaded parasites. Cells were fixed in 4% paraformaldehyde (PFA) at 24 h p.i., washed in PBS and stained with Far Red Cell Mask (1:2,000, Thermofisher Scientific). Plates were imaged on an Opera Phenix High-Content Screening System (PerkinElmer) with a 40x NA1.1 water immersion objective. 38 fields of view with 10 planes were imaged per well. Analysis was performed on a maximum projection of the planes and the percentage of infected cells was quantified over triplicate samples similarly to previously established protocols (3, 55).

Competition assay. 5x10^5 BMDMs were seeded in 12-well plates in working media. The following day cells were either treated with 100 U/ml IFN-γ or left untreated. 24 h post treatment BMDMs were infected with a 1:1 mix of either WT (PruΔKU80) and PruΔGRA12::mCherry parasites or WT and PruΔMYR1::mCherry parasites at a MOI of 0.3 (1.5x10^5 parasites per well). Confluent HFFs in 12-well plates were similarly infected to evaluate defects in growth of the KO parasites. A sample of input parasites were fixed in 4% PFA to verify the starting ratio. 48 h p.i. cells were scraped and passed through a 27G needle, and the parasites inoculated onto HFF monolayers and grown for a further 3-4 days. For flow cytometry analysis, cells were lysed with 23G needles and the parasites passed through a 5 µm filter before fixation in 4% PFA and staining with Hoechst 33342 (Thermofisher Scientific). Samples were analysed on a BD LSR Fortessa flow cytometer and with FlowJo software v10. Hoechst 33342 was excited by a 355 nm laser and detected by a 450/50 band pass filter. mCherry was excited by a 561 nm laser and detected by a 600 long pass filter and a 610/20 band pass filter. To eliminate debris from the analysis, events were gated on forward scatter, side scatter and Hoechst 33342 fluorescence. Parasites were identified by their nuclear staining and KO were discriminated by their mCherry signal. The ratios of KO/WT parasites ($mCherry^+$/ $mCherry^-$) from two independent experiments, each in technical triplicates for each condition, were calculated and normalised by dividing by the input ratio, to allow comparison between strains and biological replicates.

Plaque assay. HFF were grown to confluency in T25 flasks and infected with 200 parasites to grow undisturbed for 10 days. Cells were fixed and stained in a solution with 0.5% (w/v) crystal violet (Sigma), 0.9% (w/v) ammonium oxalate (Sigma), 20% (v/v) methanol in distilled water, then washed with tap water. Plaques were imaged on a ChemiDoc imaging system (BioRad) and measured in FIJI (56).

Animal Ethics Statement. C57BL/6J (Jackson Laboratories), C57BL/6NTac and Rag2 N12 C57BL/6N (Rag2-deficient; *Rag2*$^{-/-}$, Taconic) mice were bred and housed under specific pathogen-free conditions in the biological research facility at the Francis Crick Institute. Mice maintenance and handling adhered to the Home Office UK Animals Scientific Procedures Act 1986. All work and procedures performed were approved by the UK Home Office and performed in accordance with the granted Project License (P1A20E3F9), the Francis Crick Institute Ethical Review Panel, and conforms to European Union directive 2010/63/EU.

***In vivo* infections.** Male and female mice, aged 6-12 weeks were used in this study. For experiments, animals were sex- and age-matched. Mice were injected intraperitoneally (i.p.) with a total of 25,000 *Toxoplasma gondii* tachyzoites in 200 µL PBS either as a single-strain inoculum (100% PruΔUPRT::LucHA or

PruΔMYR1::LucHA), or as a mixed strain inoculum including 5,000 tachyzoites of luciferase-expressing strain PruΔMYR1::LucHA::mCherry (20%) and 20,000 tachyzoites of PruΔKU80 or PruΔMYR1::mCherry strains (80%). Mice were monitored and weighed regularly throughout the experiments. Parasite *in vivo* growth was monitored by intravital imaging (IVIS) at days 3, 5 and 7 p.i. Mice were injected i.p. with 100 µL of 30 mg/ml luciferin (PerkinElmer) in PBS and were anaesthetised (isoflurane 5% for induction and 2.5% afterwards) 15 min prior to bioluminescent imaging on an IVIS Spectrum CT (Perkin-Elmer). Animals were euthanised at day 7 p.i. or at humane endpoints, blood was collected by cardiac puncture and peritoneal exudate cells were harvested by peritoneal lavage through injection of 1 mL PBS i.p. Blood was transferred to serum separating tubes and centrifuged at 10,000 rpm for 10 min at 4°C to isolate serum, and peritoneal exudate was spun at 500 *g* for 5 min to remove the cellular component. IL-12p40 (#88-7120-88), TNF (#88-7324-88), IFN-γ (#88-7314-88) and CCL2/MCP-1 (#88-7391-88) levels were detected on serum and/or in suspension at peritoneal exudates of infected mice by ELISA, following manufacturer's protocol (Thermofisher). To confirm cyst formation, the brain of mice surviving infection with PruΔMYR1::LucHA::mCherry tachyzoites were homogenised in 1 mL PBS and 300 µL of the sample were stained with FITC-conjugated Dolichos Biflorus Agglutinin (DBA; 1: 200; Vector Laboratories #RL-1031) for 1 h at room temperature. Fluorescently labelled cysts were counted using a Ti-E Nikon microscope.

Data analysis. Data was analysed in GraphPad Prism v10. All data shown is presented as means ± SEM, except for violin plots, where median and quartiles are presented. Two-tailed unpaired Welch's t-test (Gaussian-distributed data) or Mann-Whitney test (non-Gaussian-distributed data) were used for statistical analysis of data with only two experimental groups. For analysis of data with three or more experimental groups, One-way or Two-way ANOVA were performed. When datasets did not follow a Gaussian distribution, data was transformed to a logarithmic scale and parametric statistical analysis was performed on transformed datasets (57). If logarithmic-transformed data still did not follow a Gaussian distribution, untransformed data was analysed by non-parametric tests (standard or multiple Mann-Whitney tests). Statistical significance was set as: ns – not statistically significant, * $p < 0.05$; ** $p < 0.01$; *** $p < 0.001$, **** $p < 0.0001$.

Author Contributions. Conceptualisation: F.T., D.F., J.C.Y., M.T.; investigation: F.T., D.F., J.C.Y., S.B.; writing, review, editing: all authors; supervision: M.T.; funding acquisition: F.T., M.T.

Acknowledgments. We thank Jeanette Wagener and Aïcha Stierlen for their help in experiment performance and setup. We thank Andreas Wack's lab for providing

protocols and support. We want to thank all members of the Treeck lab for critical and continuous discussion. This work was supported by an award to M.T. from the Wellcome Trust (223192/Z/21/Z), by funding to M.T. from the Francis Crick Institute, which receives its core funding from Cancer Research UK (CC2132 & CR2023/030/2132), the UK Medical Research Council (CC2132& CR2023/030/2132), and the Wellcome Trust (CC2132& CR2023/030/2132). MT is also supported by the FCT - Fundação para a Ciência e Tecnologia, I.P. through project reference 2023.06167.CEECIND. We thank the High-Throughput Screening Science Technology Platform (STP), the Flow Cytometry STP, the Biological Research Facility and the Imaging STP for support. The Science Technology Platforms at the Francis Crick Institute receive funding from Cancer Research UK (CC0199), the UK Medical Research Council (CC0199), and the Wellcome Trust (CC0199). F.T. is supported by the Deutsche Forschungsgemeinschaft (TO 1349/1-1). J.C.Y. is funded by an MRC Career Development award (MR/V03314X/1). We thank VEuPathDB (58) for providing access to the *Toxoplasma* databases.

Competing interests. The authors declare no competing interests.

REFERENCES

1. C. Bock, *et al.*, High-content CRISPR screening. *Nature reviews. Methods primers* **2** (2022).

2. J. Young, *et al.*, A CRISPR platform for targeted in vivo screens identifies Toxoplasma gondii virulence factors in mice. *Nat Commun* **10**, 3963 (2019).

3. S. Butterworth, *et al.*, Toxoplasma gondii virulence factor ROP1 reduces parasite susceptibility to murine and human innate immune restriction. *PLoS Pathog* **18**, e1011021 (2022).

4. G. Pappas, N. Roussos, M. E. Falagas, Toxoplasmosis snapshots: global status of Toxoplasma gondii seroprevalence and implications for pregnancy and congenital toxoplasmosis. *Int J Parasitol* **39**, 1385–94 (2009).

5. J. P. Dubey, D. S. Lindsay, C. A. Speer, Structures of Toxoplasma gondii tachyzoites, bradyzoites, and sporozoites and biology and development of tissue cysts. *Clin Microbiol Rev* **11**, 267–99 (1998).

6. M. Sasai, M. Yamamoto, Innate, adaptive, and cell-autonomous immunity against Toxoplasma gondii infection. *Exp Mol Med* **51**, 1–10 (2019).

7. R. T. Gazzinelli, *et al.*, Parasite-induced IL-12 stimulates early IFN-gamma synthesis and resistance during acute infection with Toxoplasma gondii. *J Immunol* **153**, 2533–43 (1994).

8. J. P. Saeij, E.-M. Frickel, Exposing Toxoplasma gondii hiding inside the vacuole: a role for GBPs, autophagy and host cell death. *Curr Opin Microbiol* **40**, 72–80 (2017).

9. J. D. MacMicking, Interferon-inducible effector mechanisms in cell-autonomous immunity. *Nat Rev Immunol* **12**, 367–82 (2012).

10. J. P. Hunn, C. G. Feng, A. Sher, J. C. Howard, The immunity-related GTPases in mammals: a fast-evolving cell-autonomous resistance system against intracellular pathogens. *Mamm Genome* **22**, 43–54 (2011).

11. L. D. Sibley, L. B. Adams, Y. Fukutomi, J. L. Krahenbuhl, Tumor necrosis factor-alpha triggers antitoxoplasmal activity of IFN-gamma primed macrophages. *J Immunol* **147**, 2340–5 (1991).

12. J. A. Langermans, *et al.*, IFN-gamma-induced L-arginine-dependent toxoplasmastatic activity in murine peritoneal macrophages is mediated by endogenous tumor necrosis factor-alpha. *J Immunol* **148**, 568–74 (1992).

13. A. Sher, I. P. Oswald, S. Hieny, R. T. Gazzinelli, Toxoplasma gondii induces a T-independent IFN-gamma response in natural killer cells that requires both adherent accessory cells and tumor necrosis factor-alpha. *J Immunol* **150**, 3982–9 (1993).

14. P. M. Robben, M. LaRegina, W. A. Kuziel, L. D. Sibley, Recruitment of Gr-1+ monocytes is essential for control of acute toxoplasmosis. *J Exp Med* **201**, 1761–9 (2005).

15. I. R. Dunay, *et al.*, Gr1(+) inflammatory monocytes are required for mucosal resistance to the pathogen Toxoplasma gondii. *Immunity* **29**, 306–17 (2008).

16. J. de D. Ruiz-Rosado, *et al.*, MIF Promotes Classical Activation and Conversion of Inflammatory Ly6C(high) Monocytes into TipDCs during Murine Toxoplasmosis. *Mediators Inflamm* **2016**, 9101762 (2016).

17. R. S. Goldszmid, *et al.*, NK cell-derived interferon-γ orchestrates cellular dynamics and the differentiation of monocytes into dendritic cells at the site of infection. *Immunity* **36**, 1047–59 (2012).

18. K. Barylyuk, *et al.*, A Comprehensive Subcellular Atlas of the Toxoplasma Proteome via hyperLOPIT Provides Spatial Context for Protein Functions. *Cell Host Microbe* **28**, 752-766.e9 (2020).

19. M.-A. Hakimi, P. Olias, L. D. Sibley, Toxoplasma Effectors Targeting Host Signalling and Transcription. *Clin Microbiol Rev* **30**, 615–645 (2017).

20. M. Franco, *et al.*, A Novel Secreted Protein, MYR1, Is Central to Toxoplasma's Manipulation of Host Cells. *mBio* **7** (2016).

21. M. W. Panas, J. C. Boothroyd, Toxoplasma Uses GRA16 To Upregulate Host c-Myc. *mSphere* **5** (2020).

22. N. D. Marino, *et al.*, Identification of a novel protein complex essential for effector translocation across the parasitophorous vacuole membrane of Toxoplasma gondii. *PLoS Pathog* **14**, e1006828 (2018).

23. M. W. Panas, *et al.*, Translocation of Dense Granule Effectors across the Parasitophorous Vacuole Membrane in Toxoplasma-Infected Cells Requires the Activity of ROP17, a Rhoptry Protein Kinase. *mSphere* **4** (2019).

24. A. M. Cygan, *et al.*, Coimmunoprecipitation with MYR1 Identifies Three Additional Proteins within the Toxoplasma gondii Parasitophorous Vacuole Required for Translocation of Dense Granule Effectors into Host Cells. *mSphere* **5** (2020).

25. L. O. Sangaré, *et al.*, In Vivo CRISPR Screen Identifies TgWIP as a Toxoplasma Modulator of Dendritic Cell Migration. *Cell Host Microbe* **26**, 478-492.e8 (2019).

26. P. Olias, R. D. Etheridge, Y. Zhang, M. J. Holtzman, L. D. Sibley, Toxoplasma Effector Recruits the Mi-2/NuRD Complex to Repress STAT1 Transcription and Block IFN-γ-Dependent Gene Expression. *Cell Host Microbe* **20**, 72–82 (2016).

27. G. Gay, *et al.*, Toxoplasma gondii TgIST co-opts host chromatin repressors dampening STAT1-dependent gene regulation and IFN-γ–mediated host defenses. *Journal of Experimental Medicine* **213**, 1779–1798 (2016).

28. M. W. Panas, A. Naor, A. M. Cygan, J. C. Boothroyd, Toxoplasma Controls Host Cyclin E Expression through the Use of a Novel MYR1-Dependent Effector Protein, HCE1. *mBio* **10** (2019).

29. L. Braun, *et al.*, The Toxoplasma effector TEEGR promotes parasite persistence by modulating NF-κB signalling via EZH2. *Nat Microbiol* **4**, 1208–1220 (2019).

30. A. Rosenberg, L. D. Sibley, Toxoplasma gondii secreted effectors co-opt host repressor complexes to inhibit necroptosis. *Cell Host Microbe* **29**, 1186-1198.e8 (2021).

31. A. Bougdour, *et al.*, Host cell subversion by Toxoplasma GRA16, an exported dense granule protein that targets the host cell nucleus and alters gene expression. *Cell Host Microbe* **13**, 489–500 (2013).

32. H. He, *et al.*, Characterization of a Toxoplasma effector uncovers an alternative GSK3/β-catenin-regulatory pathway of inflammation. *Elife* **7** (2018).

631 33. L. Braun, *et al.*, A Toxoplasma dense granule protein, GRA24, modulates the early
632 immune response to infection by promoting a direct and sustained host p38
633 MAPK activation. *Journal of Experimental Medicine* **210**, 2071–2086 (2013).

634 34. A. L. Ten Hoeve, *et al.*, The Toxoplasma effector GRA28 promotes parasite
635 dissemination by inducing dendritic cell-like migratory properties in infected
636 macrophages. *Cell Host Microbe* **30**, 1570-1588.e7 (2022).

637 35. A. Naor, *et al.*, MYR1-Dependent Effectors Are the Major Drivers of a Host Cell's
638 Early Response to Toxoplasma, Including Counteracting MYR1-Independent
639 Effects. *mBio* **9** (2018).

640 36. Y. Tachibana, E. Hashizaki, M. Sasai, M. Yamamoto, Host genetics highlights IFN-
641 γ-dependent Toxoplasma genes encoding secreted and non-secreted virulence
642 factors in in vivo CRISPR screens. *Cell Rep* **42**, 112592 (2023).

643 37. C. J. Giuliano, *et al.*, CRISPR-based functional profiling of the Toxoplasma gondii
644 genome during acute murine infection. *Nat Microbiol* (2024).
645 https://doi.org/10.1038/s41564-024-01754-2.

646 38. K. D. C. Jensen, *et al.*, Toxoplasma Polymorphic Effectors Determine Macrophage
647 Polarization and Intestinal Inflammation. *Cell Host Microbe* **9**, 472–483 (2011).

648 39. B. A. Fox, *et al.*, Toxoplasma gondii Parasitophorous Vacuole Membrane-
649 Associated Dense Granule Proteins Orchestrate Chronic Infection and GRA12
650 Underpins Resistance to Host Gamma Interferon. *mBio* **10** (2019).

651 40. Y. Wang, *et al.*, Genome-wide screens identify Toxoplasma gondii determinants of
652 parasite fitness in IFNγ-activated murine macrophages. *Nat Commun* **11**, 5258
653 (2020).

654 41. S. Nishiyama, A. Pradipta, J. S. Ma, M. Sasai, M. Yamamoto, T cell-derived
655 interferon-γ is required for host defense to Toxoplasma gondii. *Parasitol Int* **75**,
656 102049 (2020).

657 42. Y. Shinkai, *et al.*, RAG-2-deficient mice lack mature lymphocytes owing to inability
658 to initiate V(D)J rearrangement. *Cell* **68**, 855–67 (1992).

659 43. H. Shi, J. G. Doench, H. Chi, CRISPR screens for functional interrogation of
660 immunity. *Nat Rev Immunol* **23**, 363–380 (2023).

661 44. E. A. Holcomb, *et al.*, High-content CRISPR screening in tumor immunology. *Front*
662 *Immunol* **13**, 1041451 (2022).

663 45. D. G. Mordue, L. D. Sibley, A novel population of Gr-1+-activated macrophages
664 induced during acute toxoplasmosis. *J Leukoc Biol* **74**, 1015–25 (2003).

46. E. N. Rudzki, *et al.*, Toxoplasma gondii GRA28 Is Required for Placenta-Specific Induction of the Regulatory Chemokine CCL22 in Human and Mouse. *mBio* **12**, e0159121 (2021).

47. S. H. Seo, S. G. Kim, J. H. Shin, D. W. Ham, E. H. Shin, Toxoplasma GRA16 Inhibits NF-κB Activation through PP2A-B55 Upregulation in Non-Small-Cell Lung Carcinoma Cells. *Int J Mol Sci* **21**, 6642 (2020).

48. S. Seizova, *et al.*, Transcriptional modification of host cells harboring Toxoplasma gondii bradyzoites prevents IFN gamma-mediated cell death. *Cell Host Microbe* **30**, 232-247.e6 (2022).

49. S. Butterworth, *et al.*, High-throughput identification of Toxoplasma gondii effector proteins that target host cell transcription. *Cell Host Microbe* **31**, 1748-1762.e8 (2023).

50. A. A. Koshy, *et al.*, Toxoplasma co-opts host cells it does not invade. *PLoS Pathog* **8**, e1002825 (2012).

51. B. A. Fox, *et al.*, Type II Toxoplasma gondii KU80 Knockout Strains Enable Functional Analysis of Genes Required for Cyst Development and Latent Infection. *Eukaryot Cell* **10**, 1193–1206 (2011).

52. B. Shen, K. M. Brown, T. D. Lee, L. D. Sibley, Efficient Gene Disruption in Diverse Strains of Toxoplasma gondii Using CRISPR/CAS9. *mBio* **5** (2014).

53. I. Coppens, *et al.*, Toxoplasma gondii sequesters lysosomes from mammalian hosts in the vacuolar space. *Cell* **125**, 261–74 (2006).

54. J. P. J. Saeij, J. P. Boyle, M. E. Grigg, G. Arrizabalaga, J. C. Boothroyd, Bioluminescence Imaging of Toxoplasma gondii Infection in Living Mice Reveals Dramatic Differences between Strains. *Infect Immun* **73**, 695–702 (2005).

55. E. J. Lockyer, *et al.*, A heterotrimeric complex of Toxoplasma proteins promotes parasite survival in interferon gamma-stimulated human cells. *PLoS Biol* **21**, e3002202 (2023).

56. J. Schindelin, *et al.*, Fiji: an open-source platform for biological-image analysis. *Nat Methods* **9**, 676–82 (2012).

57. J. H. MacDonald, *Handbook of Biological Statistics*, 3rd Ed. (Sparky House Publishing, 2014).

58. B. Amos, *et al.*, VEuPathDB: the eukaryotic pathogen, vector and host bioinformatics resource center. *Nucleic Acids Res* **50**, D898–D911 (2022).

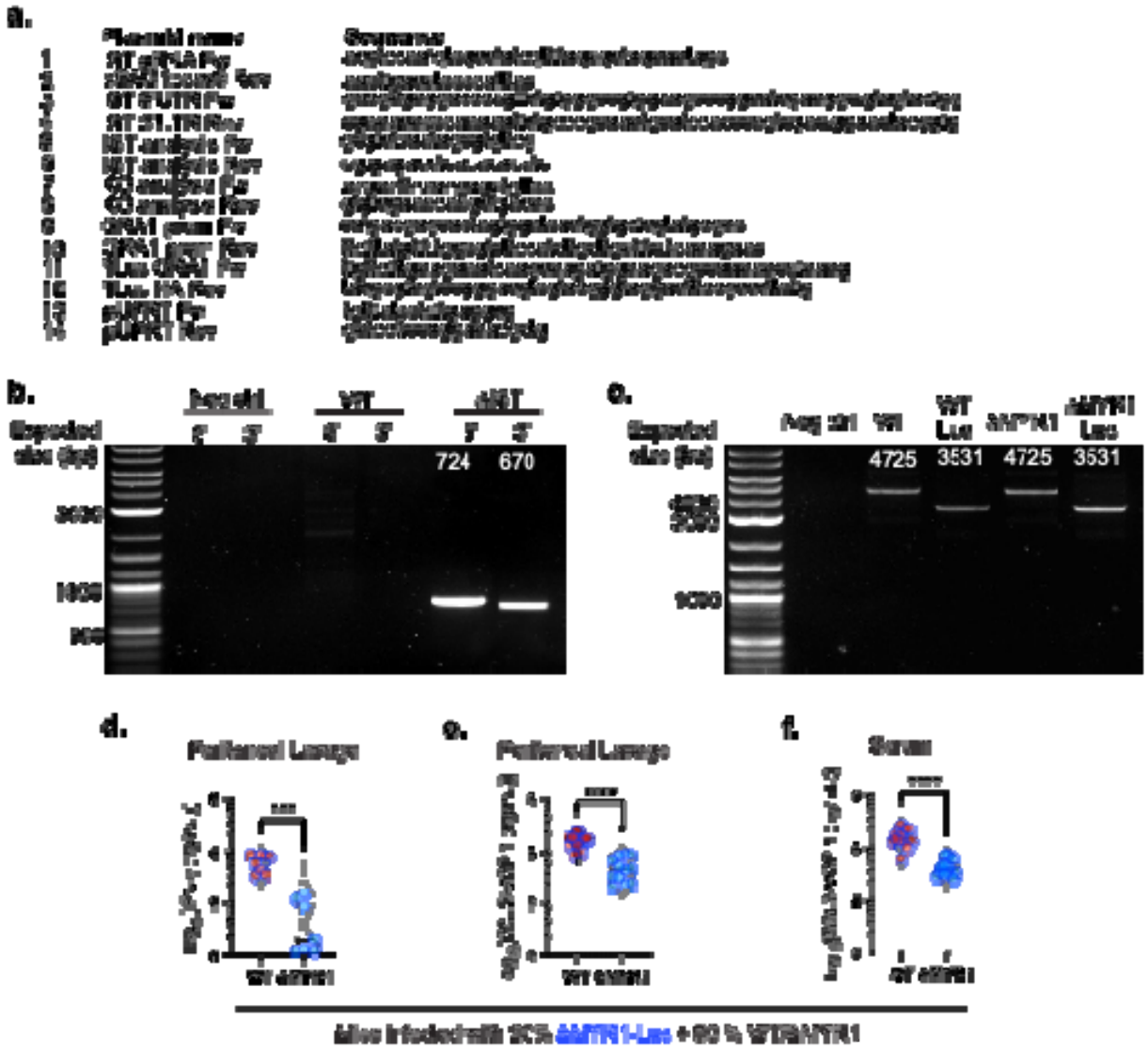

SI Appendix Fig. S1. (a) List of primers used in the study. (b) PCR validation of the PruΔIST strain compared to parental PruΔKu80 (WT). (c) PCR validation of the luciferase-expressing WT-Luc and ΔMYR-Luc strains compared to their respective parental strains PruΔKu80 (WT) and PruΔMYR1 (ΔMYR1). (d, e and f) IFN-γ at peritoneal lavage (d) and CCL2 at both peritoneal lavage (e) and serum (f), were detected by ELISA at day 7 p.i. with mixed *Toxoplasma* inocula (20:80 ratio) of luciferase-expressing ΔMYR1-Luc to WT or ΔMYR1 strains that do not express luciferase. The violin-plots display data shown in Fig. 3d converted to a logarithmic scale, with the median (continued black line) and quartile values (dotted grey lines) highlighted. Significance was tested with the Mann-Whitney test for IFN-γ, and by Welch's t-test for CCL2 data. The number of biological replicates (n) in each graph is the same as mentioned in the original graphs on Fig. 3d. *** p<0.001, **** p<0.0001.